Application of Computational Fluid Dynamics Techniques to Mitigate Wind Induced Noise in the Complex Built Environment

NEIHAD HUSSEN AL-KHALIDY
CFD, Wind and Energy,
SLR Consulting,
Tenancy 202 Submarine School, Sub Base Platypus,
120 High Street, North Sydney 2060,
AUSTRALIA

Abstract: - Wind-induced noise occurs when airflow passes through narrow architectural openings such as window interface gaps, louvres, vents, façade joints, or around elements including fins, balustrades, or decorative cladding. These interactions can generate tonal or broadband noise often perceived as whistling, humming, or howling, particularly under elevated wind conditions. This study examines the potential for wind-induced noise generated by architectural façade features and make-up air ducts provided for pressure balancing when exhaust fans operate with all other windows closed in a 29-storey mixed-use tower in Sydney. Computational Fluid Dynamics (CFD) simulations were undertaken to characterise airflow behaviour through these restricted pathways. The CFD framework predicts turbulence kinetic energy, dissipation rates, and aeroacoustic power transmitted through the gaps and around façade appurtenances. A detailed three-dimensional model of the development was constructed from architectural drawings, incorporating façade features, site topography, surrounding buildings, exhaust fans, natural ventilation plenums, and associated ductwork. The assessment required the simultaneous resolution of micro-scale airflow phenomena within millimetre-scale openings and macro-scale wind interactions across the surrounding urban environment, presenting significant numerical and modelling challenges. Simulations were performed using directional wind speeds corresponding to the 1-year return-period wind climate. A mesh-sensitivity assessment informed the adoption of a refined polyhedral mesh comprising 85,868,224 nodes to resolve complex flow structures around the openings. Multiple window-opening scenarios were evaluated, including a critical operational condition in which all windows remain closed and fresh air is supplied exclusively through a natural-ventilation make-up air duct incorporating a motorised damper with a small clearance gap. This scenario is particularly relevant for apartments exposed to elevated external noise levels where façade openings may remain closed for extended periods. The results demonstrate the effectiveness of CFD as a design tool for identifying and mitigating wind-induced noise risks, providing practical guidance for optimising façade and ventilation-system design during the early stages of project development. Such assessments remain relatively uncommon in the published literature due to the challenges associated with integrating CFD modelling, wind-engineering statistics, mechanical ventilation requirements, architectural constraints, and aeroacoustic analysis within a unified workflow. The study also discusses the numerical challenges associated with simulating coupled internal and external flows across multiple length scales, including mesh-generation requirements, solution stability, and the accurate resolution of local flow structures governing aeroacoustic source mechanisms.

Key-Words: - CFD, Wind-Induced Noise, Complex Built Environment, Apartments on Noisy Road, Coupled External and Internal Flow Assessment, Turbulence Dissipation, Acoustic Power, Make-up Air Ducts.

Received: February 6, 2026. Revised: April 5, 2026. Accepted: June 19, 2026. Published: September 17, 2026.

1 Introduction

The acoustic analogy was first formulated [1], showing that the turbulent flow can be represented as radiation from an equivalent distribution of quadrupole sources based on instantaneous velocity fluctuations. An analytical expression for the acoustic power radiated by isotropic turbulence at low Mach numbers and without mean flow was subsequently derived [2], expressing the sound intensity in terms of turbulence scales. Based on this acoustic analogy [2], the flow-induced acoustic intensity can be approximated using standard steady-state turbulence variables, namely, the turbulent kinetic energy (k) and the dissipation rate (ε). The acoustic properties of the system were investigated for the specific case where the turbulent region consists of decaying, isotropic turbulence.

The formula was later re-derived by accounting for the retarded time difference not included in original derivation, [3], [4]. Both derivations yield acoustic power (P_A) related to the unit volume of isotropic turbulence (in W/m^2) as:

$$P_A = \alpha \rho_0 \left(\frac{u^3}{l}\right) \frac{u^5}{a_0^5} \tag{1}$$

In Equation 1, u and l are the turbulence velocity (corresponding to the airflow at the gap) and length scale, respectively; a_o is the speed of sound, and α is a model constant.

Expressed in terms of kinetic energy (k) and the dissipation rate (ε), the above equation can be rewritten as:

$$P_A = \alpha_\varepsilon \rho_0 \epsilon M_t^5 \tag{2}$$

where

$$M_t = \sqrt{2k}/a_0 \tag{3}$$

α_ε is set to 0.1 based on the direct numerical simulation of isotropic turbulence reported in [5].

The acoustic power level in decibels (dB) is then computed from:

$$L_p = 10 \log \left(\frac{P_A}{P_{ref}}\right) \tag{4}$$

where P_{ref} is the standard reference pressure in air.

This formulation has been widely adopted in CFD-based aeroacoustic predictions because it allows flow-induced noise to be estimated directly from steady-state turbulence fields, avoiding the need for fully transient simulations. A computationally efficient method for estimating flow-induced noise from steady-state CFD data was proposed, [6]. The approach extends the acoustic power formulation for isotropic turbulence to non-uniform turbulent flows and expresses the acoustic spectra solely in terms of *k* and *ε*. Their approach enables practical "what-if" and optimisation studies where repeated high-fidelity Large Eddy Simulation (LES) would be prohibitively expensive.

In commercial CFD tools such as Ansys Fluent, a broadband noise source term based on the acoustic power formulation is implemented to estimate acoustic power and corresponding decibel levels reported directly from Reynolds-Averaged Navier-Stokes (RANS) turbulence fields, subject to assumptions of high Reynolds number, low Mach number, isotropic turbulence, and negligible mean flow, [7]. Broader aeroacoustic frameworks, including Lighthill-based analogies and their numerical implementation, have been extensively reviewed and refined for jet noise and general flow-generated noise prediction, highlighting the role of CFD in providing the necessary turbulence statistics, [8].

Recent CFD-focused overviews of aeroacoustics further emphasise the use of steady RANS or hybrid approaches to obtain turbulence fields, from which broadband noise metrics such as acoustic power level can be derived for engineering design applications, [9].

Broadband noise models are widely accepted for predicting wind-induced noise from gaps, fins, cladding, louvres, balustrades, and sieve plates because the dominant acoustic mechanism in these architectural features is broadband turbulence rather than strong, coherent tonal shedding. When tonal noise assessment is required, a transient CFD approach must be used. This typically involves advanced turbulence modelling such as LES or Detached Eddy Simulation (DES) to resolve periodic vortex-shedding structures, coupled with an acoustic analogy model such as the Ffowcs Williams and Hawkings (FW-H) formulation, [10]. This hybrid method enables the prediction of time- varying acoustic pressure at receiver locations and the extraction of narrow-band tonal components.

Many publications in the open literature focus on simplified geometries such as flow past cavities, jet noise, or canonical turbulent shear flows where the underlying aeroacoustic mechanisms can be isolated and studied in controlled conditions. In contrast, the present study investigates wind-induced noise for a proposed 29-storey building embedded within a complex urban built environment.

A coupled internal and external CFD model, including the macro-scale effects of the surrounding built environment, is developed to simulate airflow through narrow gaps and around architectural features, including fins, balustrades, and decorative cladding. From these simulations, the turbulent kinetic energy, dissipation rate, and corresponding aeroacoustic power are predicted using a broadband noise formulation based on the acoustic power model for turbulence, [2], [3], [4], [7]. The resulting acoustic power levels, expressed in decibels, are then evaluated to characterise the flow-induced noise associated with gap-driven and feature-driven airflow in this highly complex three-dimensional architectural context.

2 Problem Formulation

The CFD model addresses the fundamental governing equations of fluid flow, namely the continuity equation and the momentum equations. For a steady-state scenario, these equations are expressed as follows:

$$\frac{\partial}{\partial x_i}(\rho u_i) = 0 \tag{5}$$

$$\frac{\partial}{\partial x_j}(\rho u_i u_j) = -\frac{\partial p}{\partial x_i} + \frac{\partial \tau_{ij}}{\partial x_j}) + \rho g_i + F_i \tag{6}$$

In the above, ρ is the density, *u* is the velocity, *p* is the static pressure, ρg and *F* are the gravitational body and external body forces, ι_{ij} is the stress tensor. v is the kinematic viscosity.

A Realisable k-ε model is adopted to estimate the wind velocity in terms of three directions, pressure profile, and turbulence parameters. The modelled steady-state transport equations in the Realisable k-ε, [11], [12], are:

$$\frac{\partial}{\partial x_j}(\rho k u_j) = \frac{\partial}{\partial x_j}\left[(\mu + \frac{\mu_t}{\sigma_k})\frac{\partial k}{\partial x_j}\right] + G_k + G_b - \rho\varepsilon - Y_M + S_k \tag{7}$$

and

$$\frac{\partial}{\partial x_j}(\rho \varepsilon u_j) = \frac{\partial}{\partial x_j}\left[(\mu + \frac{\mu_t}{\sigma_\varepsilon})\frac{\partial \varepsilon}{\partial x_j}\right] + \rho C_1 S\varepsilon - \rho C^2 \frac{\varepsilon^2}{\mathrm{k}+\sqrt{v\varepsilon}} + C_{1\varepsilon}\frac{\varepsilon}{\mathrm{k}} C_{3\varepsilon} G_{\mathrm{b}} + S_\varepsilon \tag{8}$$

In these equations, G_K denotes the production of turbulence kinetic energy arising from mean velocity gradients, G_b signifies the generation of turbulence kinetic energy driven by buoyancy, and Y_M reflects the impact of fluctuating dilatation in compressible turbulence on the total dissipation rate, C_2 and $C_{1\varepsilon}$ are constants, and σ_k and σ_ε are the turbulent Prandtl numbers for k and ε, respectively. S denotes a user-defined source term, if required.

3 Methodology

The proposed methodology for quantitative assessment follows these key steps:

- Develop a localised wind rose tailored to the project site using long-term meteorological data to identify prevailing and extreme wind conditions relevant to the assessment.
- Construct a detailed CFD model of the proposed development, incorporating narrow architectural openings, louvres and vents, façade joints, fins, balustrades, and decorative cladding.
- Account for environmental influences, including surrounding buildings, terrain, and topography, to ensure realistic representation of windflow patterns and airflow dynamics.
- Predict wind speeds and turbulence parameters at critical locations around the development, with particular focus on gaps, façade features, and areas prone to flow acceleration or separation.
- Evaluate flow-induced noise using CFD-derived turbulence quantities and Proudman's broadband noise formulation to estimate aeroacoustics power generated by non-uniform turbulent flows.
- Recommend wind-induced noise mitigation measures and provide design guidance where required, based on the predicted noise levels and identified high-noise regions.

4 Case Study

The showcase project is located in Sydney, New South Wales (NSW), Australia, and involves the development of a 29-storey mixed-use building. The proposed design incorporates several architectural elements that influence local wind behaviour and potential wind-induced noise. These include:

- Architectural features such as wing walls and fins, which can modify façade aerodynamics and create localised flow accelerations.
- Make-up air ducts integrated into balcony façades, proposed to serve apartments adjacent to a high-traffic roadway. These ducts provide fresh air intake while also functioning as pressure-balancing pathways when exhaust fans are operating, and all other windows remain closed.

These features introduce narrow openings, façade discontinuities, and flow-sensitive geometries that warrant detailed CFD analysis to assess wind-induced turbulence, ventilation performance, and potential aeroacoustic impacts.

4.1 Local Wind Climate

The key features of Sydney's regional wind climate are illustrated by two representative wind roses shown in Figure 1, derived from Bureau of Meteorology (BoM) records collected between 1999 and 2017 at Sydney (Kingsford Smith) Airport and Bankstown Airport. Analysis of the corresponding seasonal wind roses indicates that Sydney's wind regime is characterised by two dominant wind seasons, separated by relatively short transition periods of approximately one to two months.

- Summer winds are predominantly from the northeast, southeast, and south. Northeasterly winds occur most frequently and typically manifest as offshore land-sea breezes. However, the strongest gusts during summer are more commonly associated with southeasterly and southerly winds. Northeasterly sea breezes, along with more intense southerly events such as Southerly Busters and East Coast Lows, exert a pronounced influence along the coastline. As these systems propagate inland, they generally weaken, and their directional characteristics become less distinct.
- Winter to early spring winds are dominated by westerly quadrants, with occasional contributions from the south. Westerly winds not only prevail during this season but also produce the strongest wind conditions observed throughout the year, particularly at locations situated further inland and away from coastal moderation.

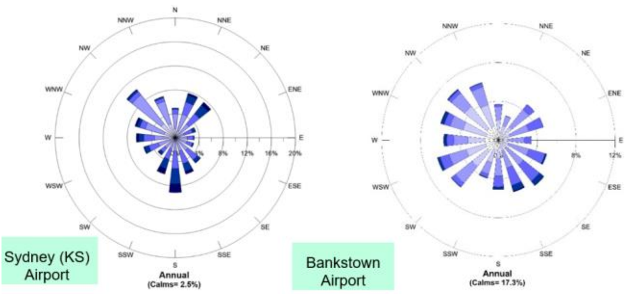

Fig. 1: Annual Wind Roses for Nearby Weather Stations: Sydney (KS) Airport and Bankstown Airport (BoM Data)
Source: developed by the author

It has been determined that local upper-level winds reflective of the weather systems experienced at the site would have characteristics closer to Bankstown Airport compared to Sydney (KS) Airport. The height design mean wind speeds (a once-per-year exceedance probability) for the site are shown in Figure 2. The highest winds occur from the west and south quadrants, with a secondary (more moderate) peak arising from summertime northeast breezes.

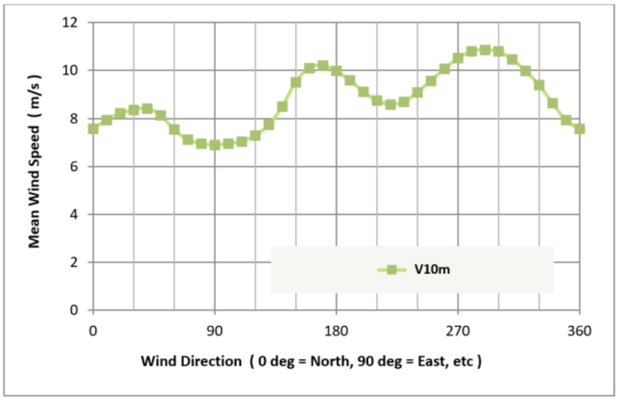

Fig. 2: Project Site 1-Year Mean Speed at 10m Height, Reference Site
Source: Developed by the author

4.2 Modelling Configuration

A detailed geometric model of the proposed development, including all architectural features at areas of interest, including the make‑ up air ducts, was developed using the SpaceClaim software package. The developed model incorporates all surrounding buildings within a 500 m radius to ensure accurate representation of the local built environment. The model also accounted for the complex site topography (refer to Figure 3). This geometry was then imported into ANSYS for mesh preparation, after which the computational model was transferred to the specialised CFD solver Ansys Fluent for numerical simulation.

The geometry was created based on the provided architectural drawings as follows:

- The model includes all facade features as per the architectural drawings given.
- The CFD model incorporates the proposed ductwork layouts on selected levels: Level 16, Level 20, and Level 25. A 3D Geometry of the proposed development is shown in Figure 4.
- Both damper states were assessed: fully open and closed. In the closed-damper scenario, it is assumed that a perfect seal is not achievable. Instead, a 4 mm clearance is applied to represent potential leakage. Figure 5 shows the geometry of a typical modelled unit, including the make-up air duct.
- Windows that do not face the adjacent noisy roadway are assumed to remain open, contributing to internal airflow distribution.

Fig. 3: CFD Simulation Domain
Source: developed by the author

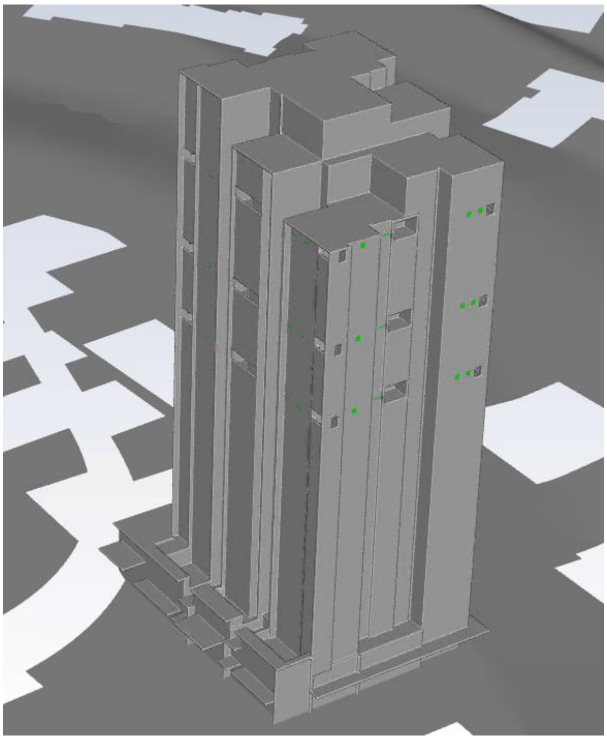

Fig. 4: 3D Geometry of the Proposed Development and Associated Make-up ducts
Source: developed by the author

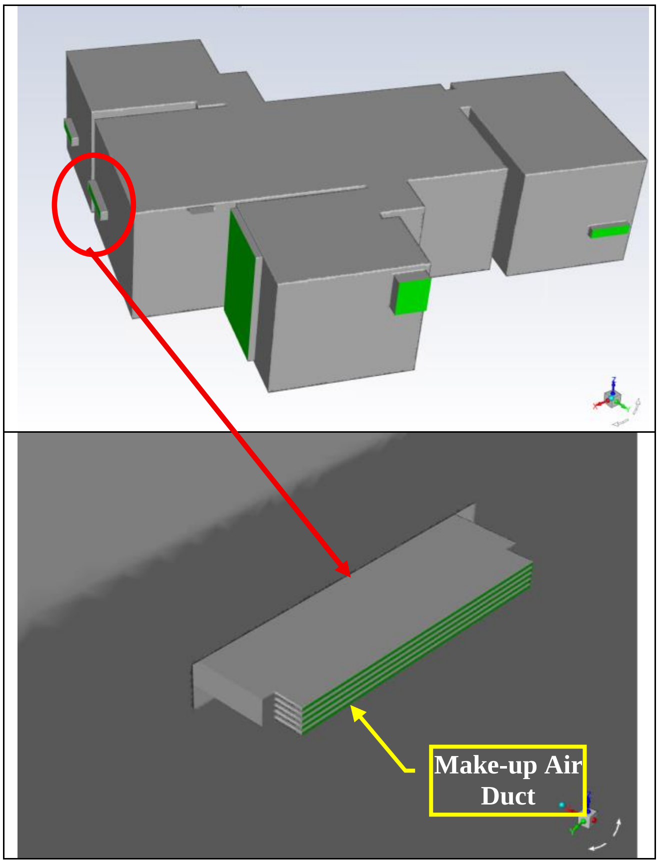

Fig. 5: 3D Geometry for a typical Unit, Level 25
Source: developed by the author

4.3 Wind Scenarios

The assessment was undertaken for all prevailing wind directions at the project site to ensure that any potential noise issues were identified and resolved during the early design stage. Sample results are presented for a selected worst-case scenario:

- South Wind = 180°

This wind direction is of primary relevance when evaluating wind-induced noise at the project site due to the orientation of the proposed development.

Velocity profiles were derived from the Australian Wind Code AS1170.2-2021 at the upwind free-boundary inlet. For example, the approaching mean wind speed for a 180° wind direction is 10.0 m/s at 10 m above ground level, with the vertical profile determined in accordance with the Terrain Category 3.0 classification specified in the Code.

The influence of terrain roughness on wind speed is then applied to determine the variation of wind speed with height.

Turbulence intensity values were adopted based on previous wind tunnel testing data undertaken for the same project.

4.4 Discretisation

The developed model represents a complex coupled internal and external flow assessment, integrating the local effects of small-scale features, such as the make-up air duct openings, architectural elements (e.g. wing walls and façade fins), and associated wind-induced noise mechanisms, with the macro-scale effects of the surrounding built environment, which provides shielding and influences the overall airflow behaviour. This integrated approach presents significant numerical challenges due to the wide range of spatial scales and flow interactions that must be accurately resolved.

The following numerical challenges are particularly relevant to achieving a reliable and robust solution:

4.4.1 Large Range of Spatial Scales and Mesh Quality Requirements

One of the primary numerical challenges in obtaining a reliable and physically realistic solution is the presence of a large range of spatial scales within the computational domain. Engineering systems often contain both large-scale flow regions and small geometric features, such as narrow gaps, sharp corners, thin boundary layers, and localised flow passages. Accurately resolving these features requires a highly refined mesh in specific regions while maintaining a manageable overall cell count.

The quality of the computational mesh plays a critical role in determining the accuracy, stability, and efficiency of the numerical simulation. Poor-quality elements, characterised by high skewness, excessive aspect ratios or non-orthogonality, can introduce significant discretisation errors.

A mesh sensitivity assessment has been carried out for the current study. A procedure has been developed to adopt very fine meshes at areas of interest. The assessment has been initially carried out using approximately 80 million mixed cells. The mesh was then converted to polyhedral elements based on the mesh sensitivity assessment. For all final cases in this study, polyhedral elements with 85,868,224 nodes were used for the final mesh scheme. Polyhedral cells are especially beneficial for handling complex flows, [13].

In summary, the mesh used in the current wind-induced noise study is significantly higher than the number of cells typically used in RANS CFD Microclimate Wind Studies. Additionally, the make-up air duct, louvres and the gaps were meticulously modelled to accurately predict turbulence levels in the areas of interest.

An example of the final mesh scheme is shown in Figure 6. The figure demonstrates that a high-quality polyhedral mesh was employed throughout the entire computational domain, with additional local refinement around the make-up air duct to accurately resolve airflow patterns and capture complex flow features in the vicinity of the opening.

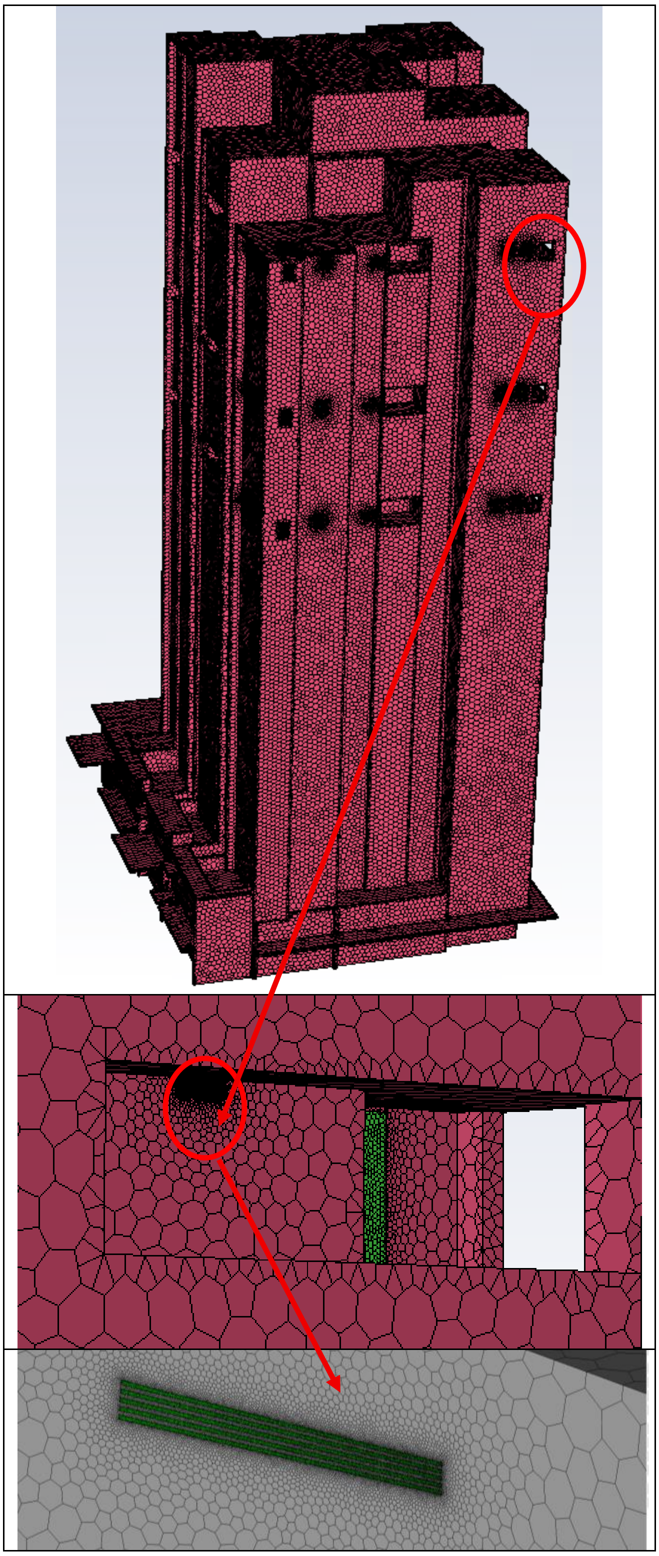

Fig. 6: Example of Mesh at the Areas of Interest
Source: developed by the author

4.4.2 Turbulence Modelling

Turbulence denotes the fluctuations which occur above and below the mean wind, both in terms of wind speed magnitude and wind direction. The turbulence level is formally the RMS (“root-mean-square”) or standard deviation of the fluctuating wind speed.

Turbulence in numerical modelling is, in principle, described by the Navier-Stokes equations. The most widely applied averaging procedure is Reynolds-averaging (which, for all practical purposes, is time-averaging) of the equations, resulting in the Reynolds-Averaged Navier-Stokes (RANS) equations. For the current study, a realisable k-epsilon (RKE) approach is used due to its ability to provide more accurate results at high pressure gradient areas.

4.4.3 Numerical Discretisation Scheme

The selection of an appropriate numerical discretisation scheme is also critical. A second-order spatial discretisation scheme is required to minimise numerical diffusion and provide improved accuracy in predicting complex flow features, including flow separation, recirculation zones, velocity gradients, and turbulence dissipation around small architectural and duct features. Lower-order schemes may artificially smooth these flow structures and potentially underpredict local turbulence levels associated with wind-induced noise

A second-order discretisation for both momentum and pressure was implemented in the current study.

Second-order schemes are essential for capturing realistic velocity, pressure, and turbulence gradients in steady-state RKE simulations, as first-order schemes often under-predict gradients, smear flow features, and can give misleadingly “stable” but inaccurate solutions.

4.4.4 Convergence and Solution Stability

The combination of complex geometry, strong pressure gradients, and separated turbulent flows can lead to slow convergence and numerical instabilities. Multiple monitoring parameters (mass balance, residual reduction, pressure stability, and key flow variables) are required to confirm solution convergence.

To enhance numerical stability and achieve convergence, appropriate under-relaxation factors were applied to the pressure, momentum and turbulence equations. The relaxation parameters were controlled to minimise numerical oscillations associated with strong pressure gradients, flow separation, and recirculation regions. The final converged solution was obtained using under-relaxation factors of 0.3, 0.32, 0.6, and 0.6 for pressure, momentum, turbulence kinetic energy, and turbulence dissipation rate, respectively.

An iterative procedure was used to estimate the air velocity in terms of three directions, pressure profile and turbulence parameters. Figure 7 shows an example of one of the simulation runs where the simulation was stopped at the desired “steady-state” outcome. The normalised residuals of continuity, volume fraction, x-, y-, and z-velocity, k and epsilon were reduced between four and nine orders of magnitude, demonstrating a valid solution.

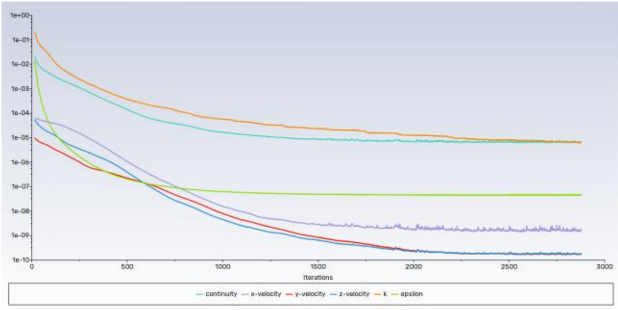

Fig. 7: Residual History
Source: developed by the author

4.5 Results and Discussion

4.5.1 The Damper of the Makeup air is Open, and Windows are Open

The CFD runs were carried out using a mean wind speed equal to the 1-year return period relevant to the simulated wind direction.

Figure 8 (Appendix) illustrates sample CFD simulation results for airflow velocity magnitudes through the makeup air ducts at Level 16 and Level 25, respectively. The velocity profiles are presented on a colour-coded scale ranging from 0 to 10 m/s, with wind speeds exceeding 10 m/s clipped for clarity and ease of interpolation. In the scale: Dark blue indicates still air at 0 m/s, and Red signifies the highest wind speeds within the displayed range.

Wind velocities in the scour regions exceed 10 m/s, indicating areas of high-speed flow beyond the upper limit of the display range.

The CFD model captures the fluid flow characteristics in significant detail. Wind approaches the site from the south as per the given boundary condition. The wind is then accelerated near the edges and penetrates the buildings through the proposed openings and the make-up air ducts.

Mean wind speeds within the level 25 duct reach approximately 5 m/s (refer to Figure 8B, Appendix).

As outlined in Section 3, elevated turbulence dissipation correlates with increased noise generation, owing to energy losses within the flow, portions of which are emitted as sound. Notably, small-scale eddies where dissipation predominantly occurs within the make-up air duct may also serve as efficient acoustic sources, particularly in the high-frequency range.

Figure 9 (Appendix) illustrates the distribution of turbulent energy dissipation rates through a 2D cross-section including the make-up air ducts at Levels 16 and 25.

Key findings from the simulation results include:

- Levels 16 and 25 exhibit similar dissipation patterns, although the magnitude varies due to differences in local façade geometry and surrounding wind exposure.
- Edge Effects from Flow Separation: Peak dissipation occurs near building edges, where substantial flow separation regions are observed.

Figure 10 (Appendix) presents the acoustic power distribution calculated from turbulence intensity levels. The following conclusions can be drawn:

- Areas exhibiting elevated turbulent kinetic energy demonstrate greater acoustic power output, indicating a strong correlation between airflow instability and sound generation.
- When windows are assumed open, reliance on make-up airflow decreases due to heightened flow resistance at the duct. The highest acoustic power level, 47 dB, is observed near the louvred inlet of a make-up air duct. Acoustic power diminishes rapidly further inside the duct (Figure 10B, Appendix).
- An acoustic power level of 42 dB is predicted near regions with strong flow separation or abrupt changes in velocity, typically occurring near the edges and wing walls, terminations and constriction points (Figure 10B, Appendix).
- The predicted acoustic power output is classified as moderate, reflecting a balanced level of sound energy under the evaluated conditions.

4.5.2 The Motorised Damper Closed, with a 4 mm Clearance Considered for Leakage Airflow and Windows and Door are Closed

For this assessment, the following assumptions were made:

- All windows are closed; fresh air supply is limited to the make-up air duct.
- External doors are assumed to be closed, with no airflow entrainment through door gaps.
- Mechanical Ventilation Rates:
  - Kitchen exhaust fan: 50 L/s
  - Bathroom exhaust fan: 30 L/s (Two fans with a total rate of 60 L/s are modelled)

Results of simulations for a selected unit are presented in Figure 11 and Figure 12 in Appendix:

The following conclusions can be reached from Figure 11 and Figure 12 in Appendix:

- The acoustic power transmitted through the make-up air duct is negligible for the open damper scenario (refer to Figure 11, Appendix), noting that all windows and sliding doors remain closed and the required mechanical exhaust ventilation rate is supplied through the open make-up air duct.
- For the closed-damper scenario, a small clearance (approximately 4 mm) allows limited airflow, given that all other openings are closed. This concentrates turbulence dissipation at the outlet of the make-up air duct, where the damper is closed. As the required mechanical ventilation rate must be supplied through these small clearances, elevated wind-induced noise levels are predicted.
- The acoustic emissions increase substantially to approximately 65 dB for the closed damper due to elevated turbulence (refer to Figure 12, Appendix).
- Further reductions in clearance are expected to intensify acoustic power output

If all windows remain closed while kitchen and bathroom fans operate simultaneously, the proposed natural ventilation make-up air system may generate audible wind-induced noise. This is attributed to fresh air being drawn through the restricted clearance around the motorised damper.

The assessment has been repeated for all prevailing wind directions at the project site to ensure that any potential noise issues are identified and resolved during the early design stage.

4.6 Recommendations

Based on the results of simulations, the following recommendations were made to reduce the wind-induced noise

- Interlock the motorised damper with exhaust fan operation. This ensures the damper opens whenever fans are active, mitigating potential wind-induced noise and improving airflow performance.

5 Conclusions

The current study provides new insights into the application of Computational Fluid Dynamics (CFD) for investigating wind-induced noise within a complex built environment. The analysis focuses on a 29-storey showcase development in Sydney, Australia, incorporating surrounding buildings, façade features, mechanical systems, and the make-up air ducts designed to enable natural ventilation for apartments located along a noisy road.

The developed coupled CFD model successfully integrates internal ventilation pathways and external wind flow effects, capturing the interaction between small-scale architectural and duct features and the surrounding built environment. Despite the numerical challenges of resolving multiple spatial scales and complex turbulent flow interactions, the methodology provides a robust framework for predicting flow features that govern wind-induced noise. The model effectively captures key aerodynamic mechanisms, including vortex generation, flow separation, and pressure fluctuations, enabling improved understanding and assessment of wind-induced noise associated with façade openings and ventilation systems.

The approach also identifies zones of elevated turbulence intensity or pressure variation that may lead to whistling, humming, or vibration-induced noise, allowing design issues to be addressed at an early stage. CFD simulations were conducted using mean wind speeds corresponding to the 1-year return period for each prevailing wind direction. A mesh-sensitivity assessment informed the adoption of a refined polyhedral mesh comprising 85,868,224 nodes, ensuring accurate resolution of complex flow structures around façade openings.

This integrated approach enables the development of targeted recommendations to mitigate wind-induced noise early in the design process, improving both acoustic performance and overall building functionality.

References:

[1] Lighthill, M., On sound generated aerodynamically, I. General theory, *Proceedings of the Royal Society of London, Series A*, Vol. 211, No. 1107, 1952, pp. 564–587. DOI: 10.1098/rspa.1952.0060.

[2] Proudman, I., The generation of noise by isotropic turbulence, *Proceedings of the Royal Society of London, Series A*, Vol. 214, 1952, pp. 119–132. DOI: 10.1098/rspa.1952.0154.

[3] Lighthill, M., On sound generated aerodynamically, II. Turbulence as a source of sound, *Proceedings of the Royal Society of London, Series A*, Vol. 222, 1954, pp. 1–32. DOI: 10.1098/rspa.1954.0049.

[4] Lilley, G., The radiated noise from isotropic turbulence revisited, NASA Contractor Report CR‐93‐75, NASA Langley Research Center, Hampton, Virginia, USA, 1993.

[5] Sarkar, S. & Hussaini, M., Computation of the sound generated by isotropic turbulence, *NASA Contractor Report CR-93-74, NASA Langley Research Center*, Hampton, Viginia, USA, 1993.

[6] Croaker, P., Skvortsov, A., & Kessissoglou, N., A simple approach to estimate flow-induced noise from steady-state CFD data, *Applied Acoustics*, 2013. DOI: 10.1016/j.apacoust.2012.06.001.

[7] ANSYS Inc., ANSYS Fluent Theory Guide: Broadband Noise Source Models – Proudman’s Formula, *ANSYS Documentation*, 2023, [Online]. https://ansyshelp.ansys.com/public/Views/Secured/corp/v251/en/flu_th/flu_th_sec_acoust_broad.html (Accessed Date: April 1, 2026).

[8] Farassat, F., & Succi, G., The Acoustic Analogy, A review of Lighthill’s Theory with Emphasis on jet noise prediction, *Journal of Sound and Vibration,* Vol. 73, 1980, pp. 483-501.

[9] Kord K, Acoustics & Aeroacoustics in CFD: The Ultimate Guide, CFD Online Technical Publication, 2021, [Online]. https://cfdland.com/acoustics-aeroacoustics-in-cfd-the-ultimate-guide (Accessed Date: April 1, 2026).

[10] Ffowcs W., & Hawkings, D., Sound Generation by Turbulence and Surfaces in Arbitrary Motion. *Philosophical Transactions of the Royal Society of London. Series A, Mathematical and Physical Sciences*, Vol. 264, No. 1151, 1969, pp.321–342.

[11] Al-Khalidy, N., On the Assessment of Wind Microclimate in a Complex Urban Environment Utilising Computational Fluid Dynamics, *WSEAS Transaction on Fluid Mechanics*, Vol. 19, 2024, pp.292-295. DOI: 10.37394/232013.2024.19.26.

[12] ANSYS. (2025). *Ansys Fluent theory manual*. USA, [Online]. https://ansyshelp.ansys.com/public/Views/Secured/corp/v252/en/flu_th/flu_th_sec_acoust_broad.html (Accessed Date: April 1, 2026).

[13] Al-Khalidy, N, Advanced Numerical Computational Fluid Dynamics Modelling for the Assessment of Potential Wind Induced Tile Uplift, *World Academy of Science Engineering and Technology*, Vol. 19, No 8, 2025, pp. 180-190.

Contribution of Individual Authors to the Creation of a Scientific Article (Ghostwriting Policy)

The author contributed to the present research, at all stages from the formulation of the problem to the final findings and solution

Sources of Funding for Research Presented in a Scientific Article or Scientific Article Itself

No funding was received for conducting this study. The original study was carried out to support a Development Application for the project site.

Conflict of Interest

The authors have no conflicts of interest to declare that are relevant to the content of this article.

APPENDIX

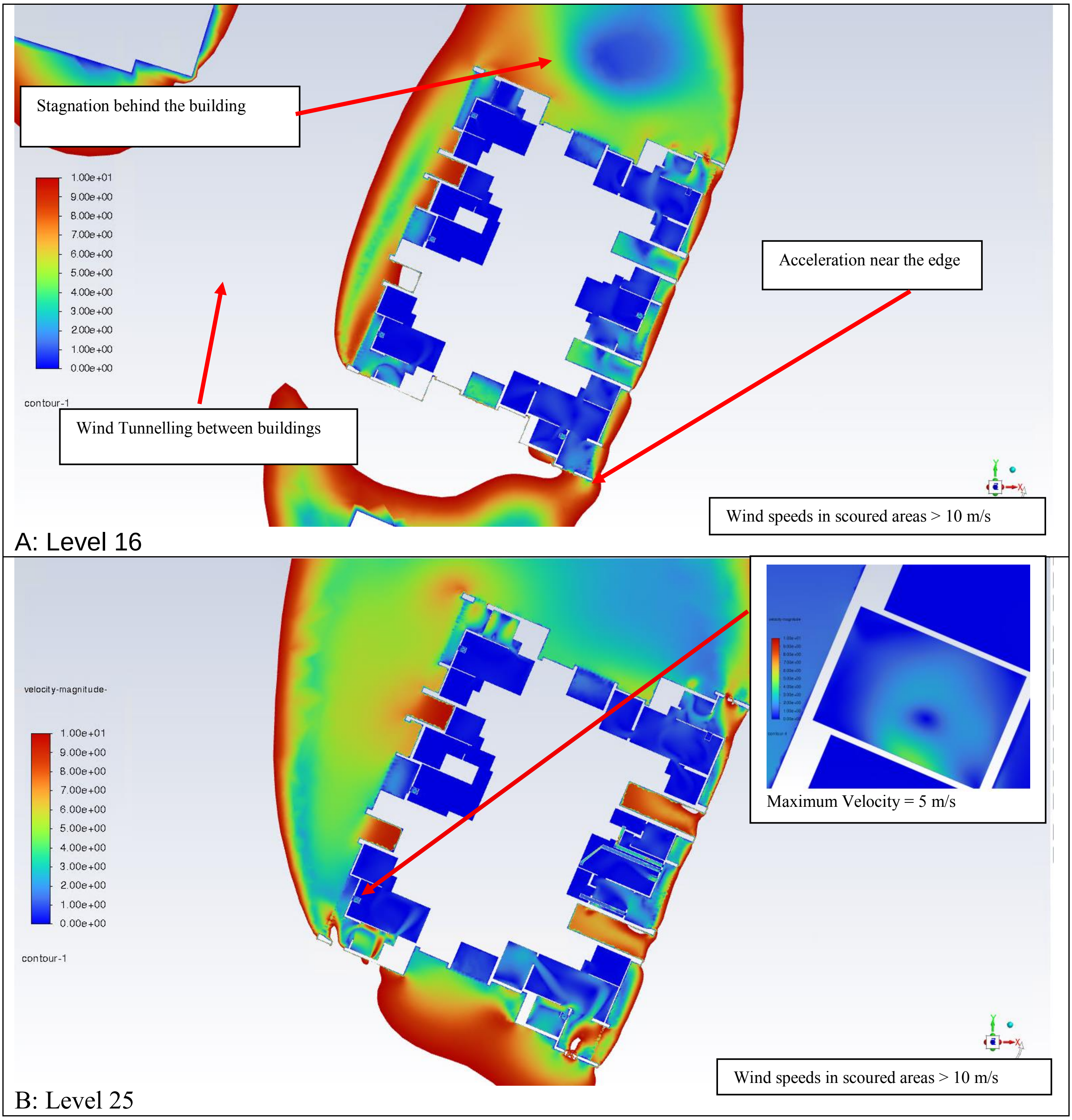

Fig. 8: Velocity Magnitudes at Selected 2D Sections through the Make-up air Ducts – Wind Angle = 180°

Source: developed by the author

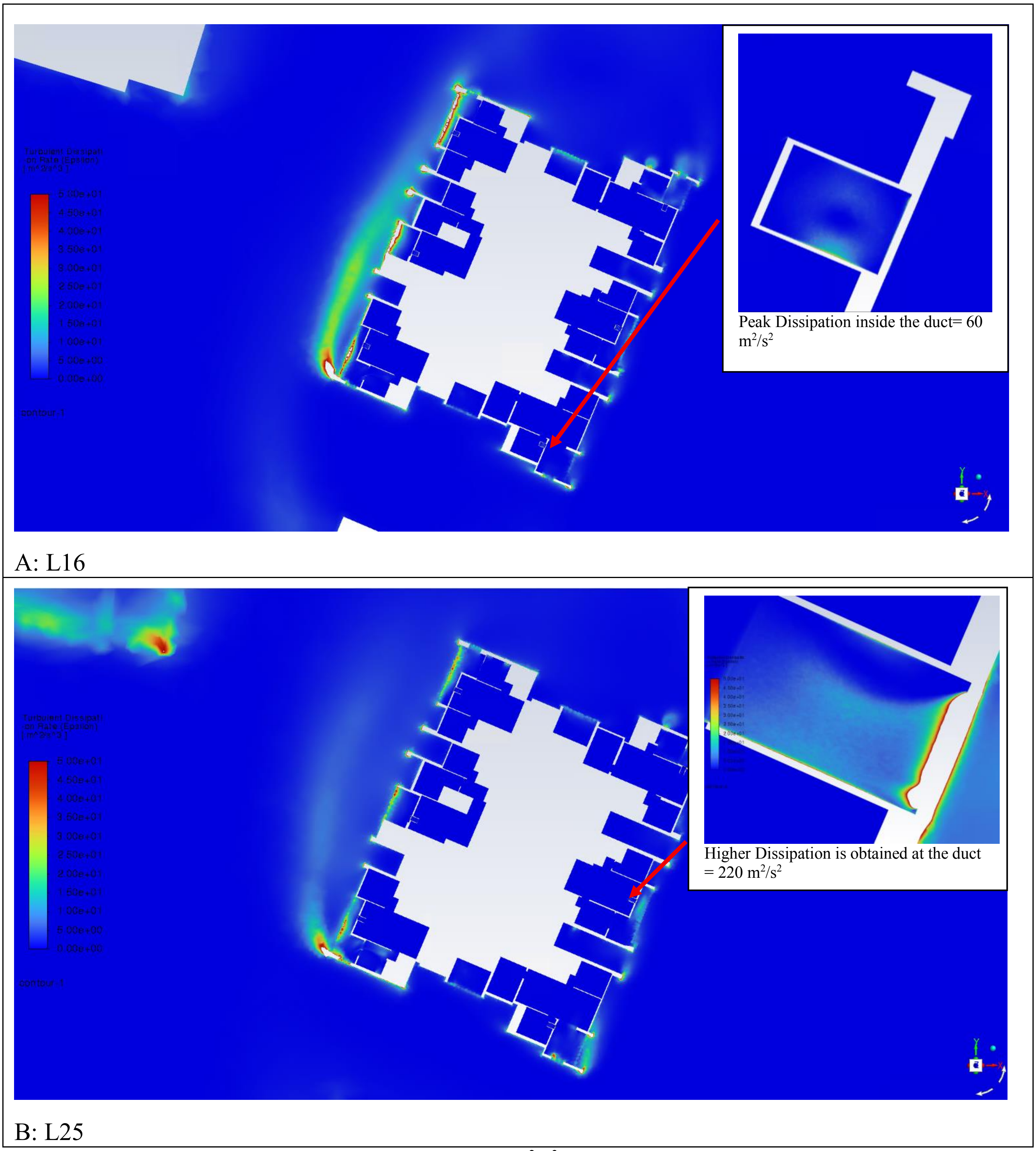

Fig. 9: Contoures of Turbulent Dissipation Rate (m^2/s^3) at Selected 2D Sections - Wind Angle = 180°
Source: developed by the author

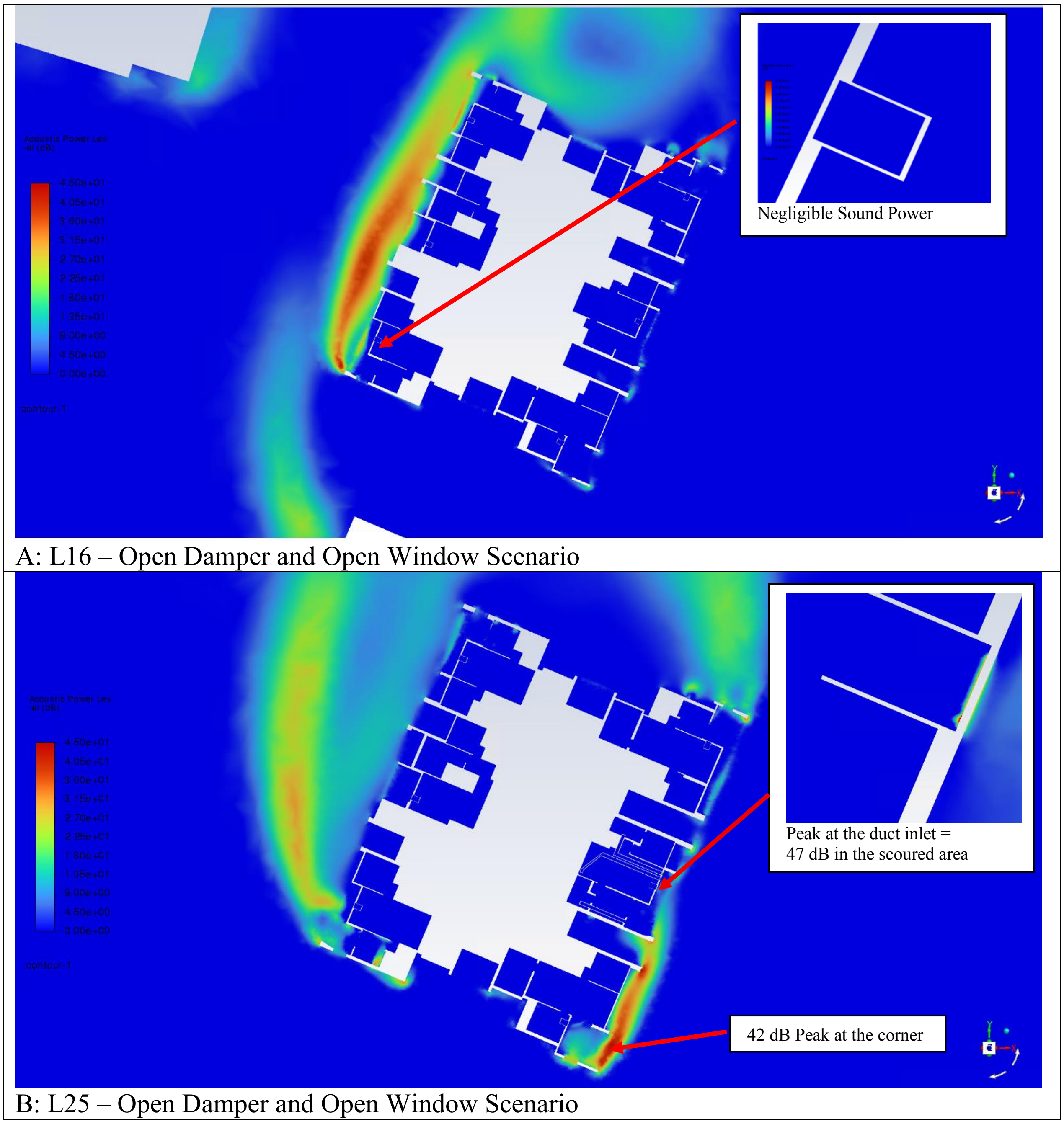

Fig. 10: Overall Acoustic Power Level (dB) – Wind Angle = 180°

Source: developed by the author

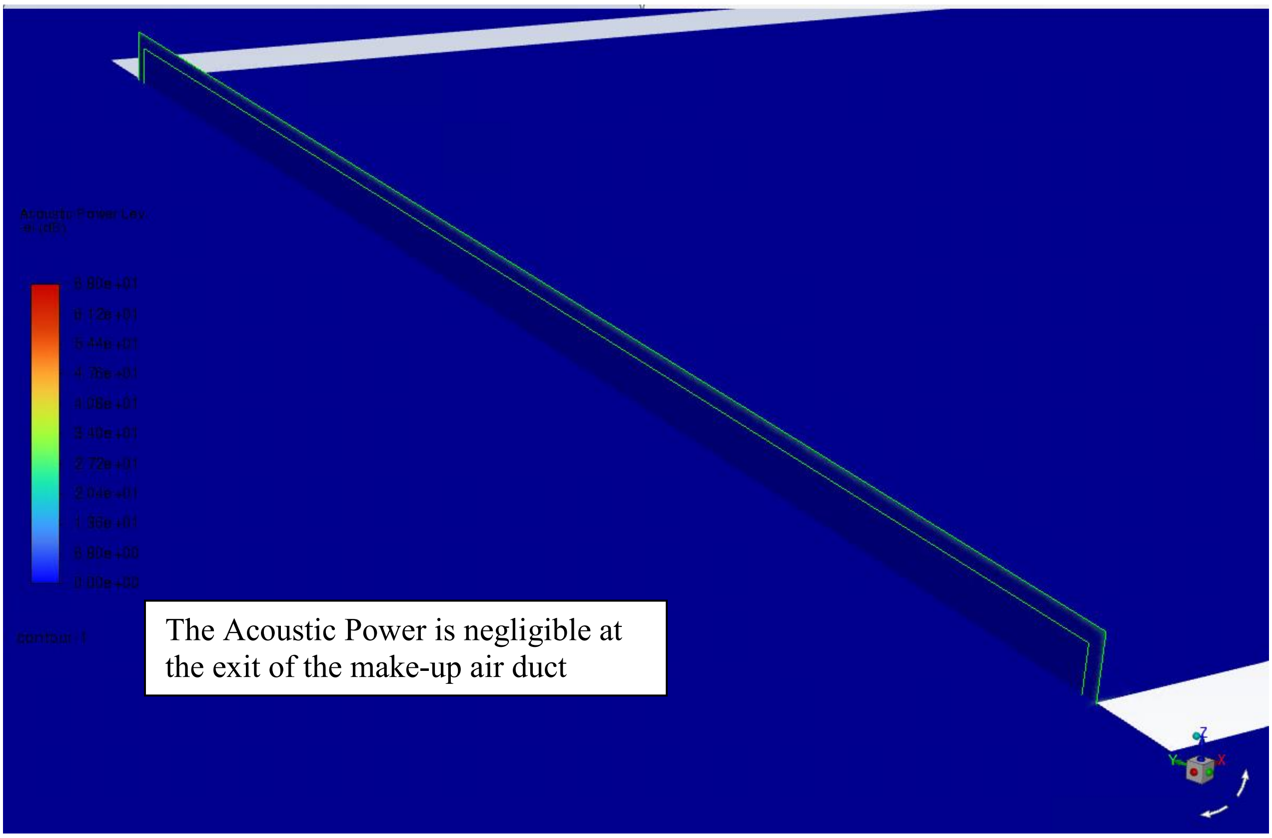

Fig. 11: Acoustic Power Level (dB) at the Exit of the Make-up Air Duct, Motorised Damper is Fully Open, Exhaust fans are operated, and ALL doors and Windows are closed

Source: developed by the author

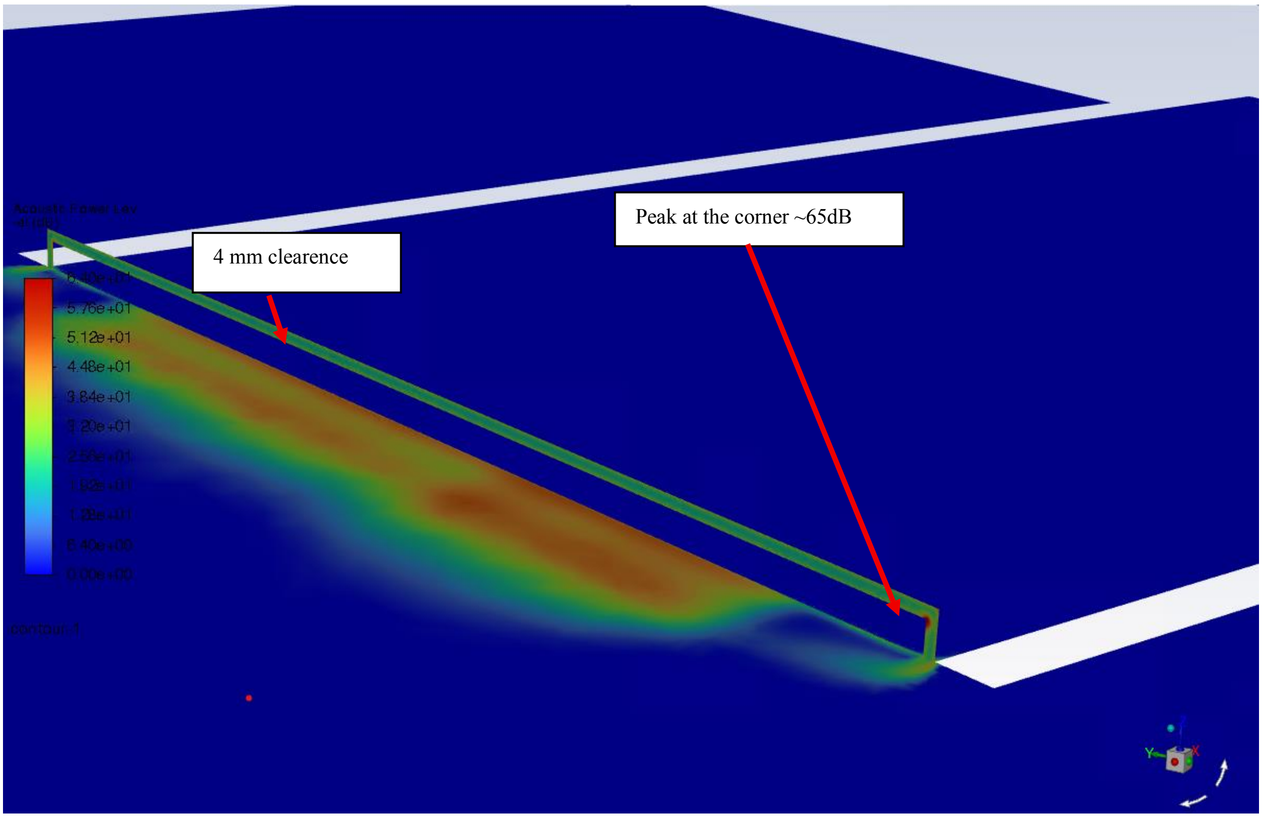

Fig. 12: Acoustic Power Level (dB) at the Exit of the Make-up Air Duct, Motorised Damper is Fully Closed, Exhaust fans are operated, and ALL doors and Windows are closed

Source: developed by the author